A study of zebrafish locomotion using experimental and numerical simulation

Zhenkai Zhao[1], Qing Xiao*, [1] Xinhua Shu[2], Gen Li[3] and Hao Liu[4, 5]

[1] Department of Naval Architecture, Ocean, and Marine Engineering, University of Strathclyde, Glasgow G4 0LZ, United Kingdom

[2] Department of Life Sciences, Glasgow Caledonian University, Glasgow G4 0BA, United Kingdom

[3]Department of Mathematical Science and Advanced Technology, Japan Agency for Marine-Earth Science and Technology (JAMSTEC), Yokohama-city, Kanagawa, Japan

[4] Graduate School of Engineering, Chiba University, 1-33, Yayoi-cho, Inage-ku, Chiba, Japan

[5] Shanghai-Jiao Tong University and Chiba University International Cooperative Research Centre (SJTU-CU ICRC), 800 Dongchuan Road, Minhang District, Shanghai, People's Republic of China

Abstract

Zebrafish larvae has aroused worldwide attention in the medical field for assisting the development of new medicines because of its biological nature. To study the interactions between swimming zebrafish and surrounding fluid, we have developed a novel tool to exploit intravital changes based on the experimentally observed zebrafish locomotion. By using our in-house MATLAB code and a customized Computational Fluid Dynamics (CFD) tool, we are able to simulate the real zebrafish swimming which is comparable to the observed live zebrafish.

Keywords: Zebrafish, FSI, forward swimming speed, locomotion

1. Introduction

The mechanism of fish swimming is a complex problem. Most of fish species swim in an efficient way by undulating their bodies rhythmically which is the so-called "body and caudal fin swimming". During fish locomotion, internal fish body muscles work together with the surrounding fluid to provide the forces for various swimming patterns. Therefore, it is intriguing to dig into the fluid and fish body interaction for a deeper understanding of the fish swimming mechanism. In the recent ten years, due to large demands in biological, medical and genetic researches, living zebrafish larvae and their computational models are used extensively. In embryo and larval stage, fish body is nearly transparent, which is very convenient for scientists to observe fish cell development. Its quick reproduction speed and relatively cheaper cost as compared to other fish species and white mouse has brought it to a position for the scientific research. Müller recorded the lateral displacement and curvature profiles of zebrafish larvae at different developmental stages for three swimming behaviors via high speed video camera [1]. The zebrafish profile and age influences on kinematic performance were discussed systematically. The results revealed that age and profile could both have a positive influence on swimming performance such as the forward swimming speed. In a subsequent paper [2], Müller *et al.* moved one step further by analyzing larva wake patterns for different swimming behaviors using two-dimensional digital particle image velocimetry (2D-DPIV) in the horizontal and transverse planes of the flow field, detecting a consistent wake pattern compared with swimming adult eels [2]

Compared with experimental flow visualizations, CFD can provide more detailed flow information. Fish larvae swimming in the intermediate flow regime experience both inertial and viscous forces, of which the Reynolds number ranges typically from 10^2 to 10^3 [3]. Different from adult fish, zebrafish larvae have to propel themselves against much more viscous drag, and consume more energy by executing larger tail-beat frequency and amplitude, which will further lead to a lower swimming efficiency and higher cost of transport. Van Leeuwen *et al.* revealed that how body dynamics and kinematics vary with Reynolds number

* Corresponding author: University of Strathclyde, Glasgow, G4 0LZ, United Kingdom (email: qing.xiao@strath.ac.uk)

and fish developmental stages [4]. Their observations elucidated the relationships between swimming speed and Strouhal number experimentally by using a customized MATLAB program.

In this study, we developed an in-house program to solve Fluid structure interaction (FSI) problem. Validations based on some previous researchers' works and comparisons between experimental results and CFD simulation will be presented. We demonstrate that our developed tool can achieve similar results compared with biology experiment observations, and can build a foundation for our future contribution to medical research field. Future research interests will be discussed as well.

2. Materials & Methods

2.1. Ethics

Animal experiments were carried out in compliance with the Animal Ethics and Welfare Committee, Department of Life Sciences, Glasgow Caledonian University, and UK Home Office under Project License PPL 60/4169.

2.2. Experiment setup & data post-processing

The experimental setup is shown in Fig.1 and methodology was explained in our previous study, where the investigation was carried out to determine the color preference on zebrafish [5]. A total of five 5 dpf (days post-fertilization) zebrafish siblings were used and swam freely in petri dish, immersed in E3 medium (5mM NaCl, 0.17mM KCL, 0.33mM $CaCl_2$, 0.22mM $MgSO_4$, and 0.1% methylene blue) containing food to keep zebrafish larvae alive. The petri dish was illuminated by a LED panel, driven by an adjustable DC power supply (CSI5003XE, Circuit Specialists, and USA) to provide a continuous and constant light. High-speed video camera (Mikrotron EoSens CL MC1362) was used to record fish swimming behaviors. The frame rate of the camera was set at 300 frame per second (fps) during the entire experiment process to convert to the time scale easier between live video and compressed output video. Water temperature was set to 27°C. Zebrafish had 10 minutes' time to swim freely to get familiar with the environment before the camera started recording.

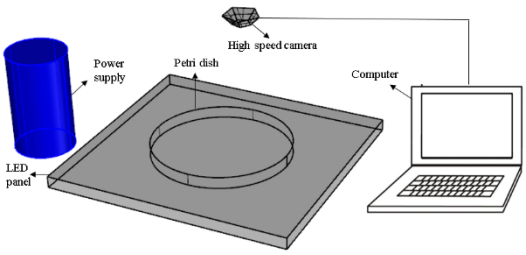

Figure 1. Experiment apparatus using high-speed camera to record the swimming behaviours of zebrafish larva.

An in-house MATLAB code was developed and used to post-process the recorded video and extract zebrafish kinematic motion equations. Key frames for the process are depicted in Fig.2 (a)-(d). As shown in Fig.2 (d), the whole fish body were divided into nine sections in order to extract eight angle functions describing the relative orientation between each two adjacent sections. The mesh around fish body is shown in Fig 2 (e). The typical example for prescribing the angle between two elements is expressed as equation (1).

$$a\cos(wt)+b\sin(wt) \qquad (1)$$

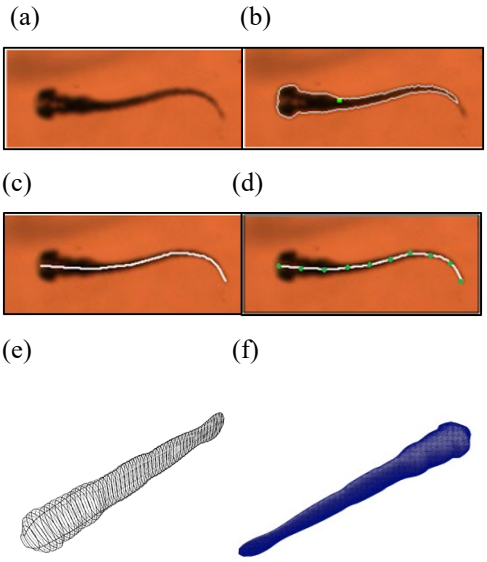

Figure 2. Key features of processed zebrafish video and CFD model. (a) Zebrafish larva captured by high speed camera; (b) zebrafish larva outline and centre of mass; (c) centre line of the zebrafish larva; (d) equal-distant points on the backbone curve; (e) 3-D fish silhouette represented with 50 ellipses.

2.3 CFD solver & dynamics motion solver

Zebrafish larva model used in OpenFOAM [6] was built with 50 ellipses extracted from real fish silhouette and rebuilt into nine sections controlled by kinematic equations as shown in Fig. 2(e). The flow field was simulated using the open source CFD toolbox OpenFOAM version 3.0.x. the 3-D computational domain was 15 times of fish body length (BL) in the longitudinal (x) direction, 10 times of BL in transverse (y) direction and 4 times of BL in perpendicular (z) direction. The overall fluid domain was assumed to be at rest initially. Considering the constraints in OpenFOAM regarding large mesh deformation to model self-propelled zebrafish swimming, a fully unstructured mesh was used to tolerate the internal mesh deformation. For ellipses with high aspect ratio, the mesh is specially refined at the tips to ensure that enough cells are existed to precisely capture the vortex at the tips.

To tackle mesh motion around zebrafish model, a modified displacementSBRStress motion solver was applied in OpenFOAM. PimpleDyMFoam solver was used to solve the transient, incompressible and single-phase Newtonian fluids. PIMPLE algorithm, a combination of SIMPLE and PISO, was used to address velocity-pressure coupling [7]. Incompressible laminar Navier-Stokes equation was written in equation (2) including the conservation equations of mass and momentum. Second-order Crank-Nicolson time marching scheme was used for temporal discretization. To ensure similar accuracy compared to structured grids, bounded second-order reconCentral limited discretization schemes were applied for convection terms in Navier-Stokes equation to improve stability and accuracy.

$$\nabla \cdot (\vec{U}) = 0$$
$$\frac{\partial \vec{U}}{\partial t} + \nabla \cdot (\vec{U}\vec{U}) = -\frac{1}{\rho} + \nabla \cdot (\upsilon \nabla \vec{U}) \qquad (2)$$

Besides OpenFOAM, a free general purpose multibody dynamics analysis software MBDyn was used to solve kinematic motion of zebrafish. The software was coupled with OpenFOAM and data was transmitted bi-directionally with Transmission Control Protocol (TCP) socket. A simple description of the process is shown in Fig. 3. MBDyn solves initial value problem in the form of Differential-Algebraic Equations (DAE), integrated in time domain using A/L-stable multi-step integration schemes [8]. Constraints can be added independently in MBDyn, both for rigid and deformed body in six degrees of freedom. Dynamics of a set of rigid bodies is written in the form of Newton-Euler equations, constrained by Lagrange's multipliers. For constrained nodes, the equations of motion are expressed as

$$M(x)\dot{x} = q$$
$$\dot{q} + \phi^{T}{}_{/x}\lambda = f(x, \dot{x}, t) \qquad (3)$$
$$\phi(x, t) = 0$$

Where x summarizes the n coordinates of the system, $M(x)$ is the mass matrix, q summarizes the momentum and momenta moments, λ represents Lagrange's multipliers, and f summarizes the generic force including pressure and viscous force.

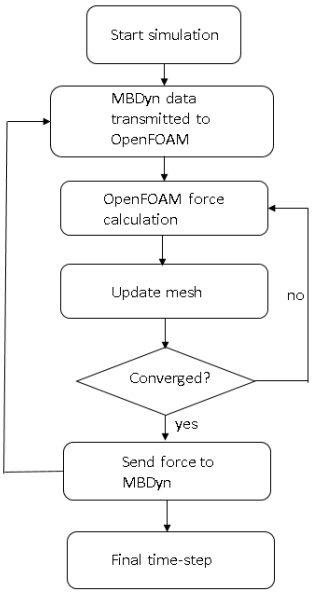

Figure 3. Schematic diagram for solid body and fluid coupling, convergence criteria is self-defined and should be satisfied before force and moment transmission

3. Results

3.1 Numerical methodology validation

The numerical coupling methodology on multi-body structure simulation was validated based on a jellyfish-inspired swimming case provided by Wilson [9]. The CFD model of jellyfish was shown in Fig. 4(a), represented by ellipses with different aspect ratios. Relative angle

functions were prescribed and expressed as $\theta_1, \theta_2, \theta_3$. By specifying those equations, the jellyfish model can move upwards with alternant contraction and refilling. In this paper, Reynolds number is defined as $Re = \frac{D^2_{\max}}{T\upsilon}$, where D is the maximum diameter of jellyfish, T is the undulation period and υ denotes kinematic viscosity. Fig.4 (b) and Fig.4(c) depict the kinematic performance of the multi-body structure with fully prescribed motion, which Fig. 4(d) illustrates the power required for the model to move cyclically. Vorticity comparison at *Re* = 140 is shown in Fig. 5(e). All of our results are in close consistent with Wilson & Eldredge's results, the small discrepancies can be caused by the different numerical methods used.

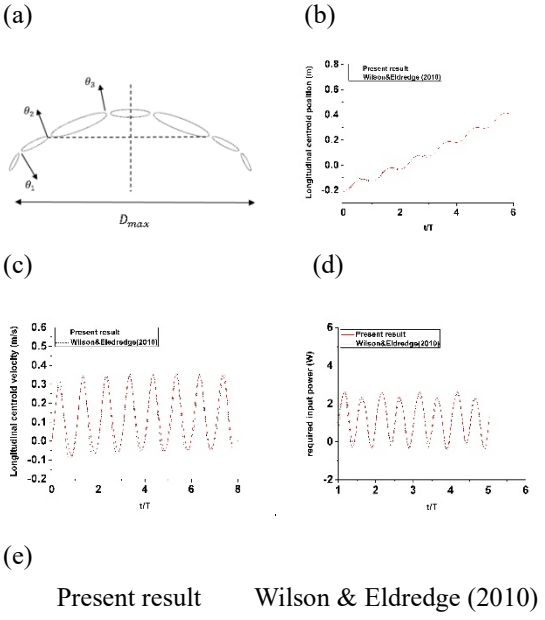

Figure 4. (a) CFD jellyfish model (b) Longitudinal centroid position for Re = 140. (c) Longitudinal centroid velocity for Re = 140. (d) Required input power for Re = 140. (e) Vorticity at Re = 140.

3.2. Comparisons between experiments and numerical simulation

As the above mentioned, in the experiment, a total of ten zebrafish larvae in the same developmental stage were tested. The body information was summarised in Table 1. For the simplicity of calculation, we assumed that the body mass and length for the ten zebrafish larvae were same. As the motion equations specify relative angle orientation, head and tail angles were calculated based on interactions with surrounding fluid. Experimental data were processed to obtain the head and tail angle and the forward swimming velocity. As shown in Fig. 5, the kinematic performance provided by CFD simulation match well with the experimental data, slight differences observed can be caused by the insufficient accuracy of fish model capturing toolbox, which might lead to little inconsistency existing in some certain captured point of head/tail angle. The forward swimming velocity experiences an acceleration stage and then reaches a swimming speed of $19.25 l_{body}/s$, which is about 95% of that in the experimentally data, this is compatible with the results shown in [10]. The small difference is noted as our CFD fish model is controlled by a prescribed motion, whereas the living fish is capable of active control, with spring-mass system built in their body, which may give them the abilities to adjust their transient bodies' curvatures to fit the environmental change. Those subtle changes cannot be captured and covered with the simplified prescribed motion equations. The forward components of total forces were illustrated in Fig. 5(d), indicating that the drag force (negative value) was mainly generated at the anterior one-third body part, whereas the thrust force (positive value) was generated in the posterior part, whose value shows a general augmentation towards the tail and stops approximately at the position of 80% body length. The five zebrafish larvae used in the experiment were numbered as one to five and expressed in terms of forward velocity and thrust power in Fig. 5(e) and Fig. 5(f), respectively.

Table 1. Detailed zebrafish larva body information

Body section number	Mass (mg)	Length (mm)
1	0.0385	0.4
2	0.0553	0.4
3	0.0425	0.48
4	0.0308	0.48
5	0.0212	0.48
6	0.019	0.48
7	0.011	0.48
8	0.009	0.48
9	0.003	0.32
Total	0.23	4

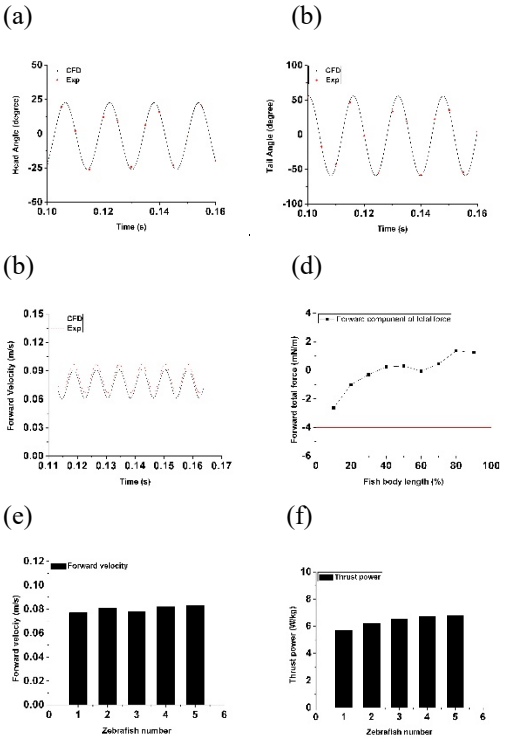

Figure 5. CFD results and comparisons with experiments. (a) Head angle comparison; (b) Tail angle comparison; (c) Forward velocity comparison; (d) Force distribution along body; (e) Forward velocity for five fish larvae; (f) Thrust power for five fish larvae

4. Conclusion

This paper has presented a multi-element tool used to unveil the real zebrafish swimming motion from the perspective of engineering science. Kinematic performance of zebrafish has been compared with experiments, while some additional information such as the thrust, the power and the force distribution along fish body were analysed based on a CFD simulation. These results verify that our developed simulation tool is able to mimic the real zebrafish motion on the whole, which makes it possible to reflect the intravital changes associated with real fish in future application.

5. Reference

[1]. Muller, U.K., Swimming of larval zebrafish: ontogeny of body waves and implications for locomotory development. The Journal of Experimental Biology, 2004. **207**(5): p. 853-868.

[2]. Muller, U.K., J.G. van den Boogaart, and J.L. van Leeuwen, Flow patterns of larval fish: undulatory swimming in the intermediate flow regime. The Journal of Experimental Biology, 2008. **211**(Pt 2): p. 196-205.

[3]. McHenry, M.J. and G.V. Lauder, The mechanical scaling of coasting in zebrafish (Danio rerio). The Journal of Experimental Biology, 2005. **208**(Pt 12): p. 2289-301.

[4]. van Leeuwen, J.L., C.J. Voesenek, and U.K. Muller, How body torque and Strouhal number change with swimming speed and developmental stage in larval zebrafish. J R Soc Interface, 2015. **12**(110): p. 0479.

[5]. Jia, L., R.K. Raghupathy, A. Albalawi, Z. Zhao, J. Reilly, Q. Xiao, and X. Shu, A colour preference technique to evaluate acrylamide-induced toxicity in zebrafish. Comp Biochem Physiol C Toxicol Pharmacol, 2017. **199**: p. 11-19.

[6]. OpenFOAM. The OpenFOAM website [OL] http://www.openfoam.com/.

[7]. Liu, Y., Q. Xiao, A. Incecik, C. Peyrard, and D. Wan, Establishing a fully coupled CFD analysis tool for floating offshore wind turbines. Renewable Energy, 2017. **112**: p. 280-301.

[8]. Li, Y., Coupled Computational fluid dynamics/multibody dynamics method with application to wind turbine simulations. Lowa Research online, 2014.

[9]. Wilson, M.M. and J.D. Eldredge, Performance improvement through passive mechanics in jellyfish-inspired swimming. International Journal of Non-Linear Mechanics, 2011. **46**(4): p. 557-567.

[10]. Li, G., U.K. Muller, J.L. van Leeuwen, and H. Liu, Fish larvae exploit edge vortices along their dorsal and ventral fin folds to propel themselves. J R Soc Interface, 2016. **13**(116).